

Fuzzy time series forecasting of nonstationary wind and wave data

Christos Stefanakos^{a,*}

^a*SINTEF Materials and Chemistry, Department of Environmental Technology - Monitoring and Modelling, P.O. Box 4760 Sluppen, NO-7465, Trondheim, Norway*

Abstract

In this paper, the well-known Fuzzy Inference Systems (FIS) in combination with Adaptive Network-based Fuzzy Inference Systems (ANFIS) are coupled for the first time with a nonstationary time series modelling for an improved prediction of wind and wave parameters. The data set used consists of ten-year long three-hourly time series of significant wave height H_S , peak wave period T_p and wind speed W_S based on hindcasts of WAVEWATCH III model and GFS analysis winds. The field used covers the area $[30W,40E] \times [50N,78N]$. The initial time series is first decomposed by means of the aforementioned nonstationary modelling into a seasonal mean value and a residual time series multiplied by a seasonal standard deviation. Then, the FIS/ANFIS models are applied to the stationary part only in order to calculate forecasts of future values. Using the nonstationary modelling, forecasts of the full time series are finally obtained. For comparison purposes, the FIS/ANFIS models are also applied to the initial nonstationary series. The performance of both forecasting procedures is assessed by means of well-known error measures. The methodology is applied to obtain a) point-wise forecasts for a specific datapoint, and b) field-wise forecasts for the whole field of wave parameters. Especially, the latter is performed for the first time. The comparison of the error measures from the two approaches showed that the forecasts based on the proposed methodology outperforms the ones

*Corresponding author

Email address: `christos.stefanakos@sintef.no` (Christos Stefanakos)

using only FIS/ANFIS models.

Keywords: fuzzy time series, significant wave height, peak wave period, wind speed, forecasting, prediction error

1. Introduction

Wind and wave data are very important for a number of applications, including among others design of coastal and offshore structures, coastal erosion and sediment transport, wave energy resource evaluation etc.

In situ buoy measurements consist the most reliable data source. However, measurement campaigns are considerably costly, and buoy networks do not have a good spatial coverage of the seas, providing us with a relatively small number of long-term records of wind and wave measurements. A very useful alternative is the long-term hindcast wave databases based on third generation spectral wave models (The WAMDI Group, 1988; Tolman, 1991; Booij et al., 1999). They provide us with data of good spatial and time resolution without gaps, and, thus, can be used for forecasting purposes (either off-line or in near real-time); see, e.g., Roulston et al. (2005); Reikard & Rogers (2011). However, and because their numerical implementation is quite complicated, they require great computational power and high CPU time.

On the other hand, various researchers treat the forecasting problem by means of various soft computing techniques (Mahjoobi et al., 2008). Some of them utilize Artificial Neural Networks (ANN); see, e.g., Deo et al. (2001); Rao & Mandal (2005); Jain & Deo (2007). Some others use Fuzzy Inference Systems (FIS) in combination with Adaptive Network-based Fuzzy Inference Systems (ANFIS). Kazeminezhad et al. (2005) developed an ANFIS model for the prediction of wave parameters (height and period) based on past wind parameters (speed, fetch) and applied his findings to data from lake Ontario. Özger & Şen (2007) applied ANFIS to buoy data from the west American coast (off California) to predict wave data based on a combination of past values of both wind and wave data. See also Zamani et al. (2008); Sylaios et al. (2009); Akpinar et al.

(2014), who presented various different ANFIS approaches for the prediction of wave parameters using buoy data from the Caspian, Aegean and Black Sea, respectively. It should be noted that ANFIS techniques require less computational effort and they are easy to be applied.

In the present work, FIS and ANFIS models are combined for the first time with a nonstationary (NS) modelling in the prediction of wind and wave parameters. NS model has been developed by the author in a series of works for the analysis, modelling and simulation of wind and wave parameters (Athanasoulis & Stefanakos, 1995; Stefanakos & Belibassakis, 2005, and references cited therein), and recently of bunker prices (Stefanakos & Schinas, 2014). Here, it is used for the extraction of the nonstationary character of the data, and then FIS/ANFIS models are applied only to the stationary part. As it will be shown in the sequel, this step is essential for the accuracy of the prediction models. Forecasting procedures are tested against model data from the North Atlantic Ocean both on a point- and a field-wise basis. The quality of the forecasts is tested against estimates obtained by applying FIS/ANFIS models to the initial nonstationary series. Especially field results, i.e. forecasts for a large area in the Atlantic Ocean, are presented for the first time depicting the great potential usability of the prediction model.

2. The nonstationary stochastic model

The nonstationary stochastic model under discussion in the present work has been presented in its univariate form in Athanassoulis & Stefanakos (1995), and been extended to its multivariate version in Stefanakos & Belibassakis (2005); see also Stefanakos & Schinas (2014). It can be described as follows; see also Fig.1.

A many-year long time series of wind and wave data can be treated as a nonstationary stochastic process with yearly periodic mean value and standard deviation. That is, it admits of the following decomposition:

$$Y(t) = m(t) + s(t) W(t), \tag{1}$$

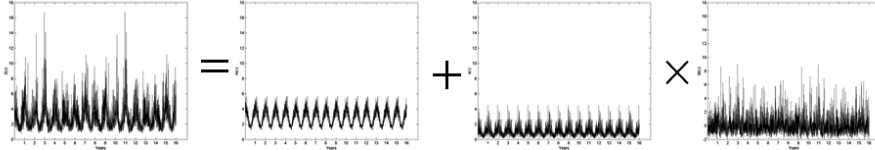


Figure 1: Nonstationary time series modelling

where $m(t)$ and $s(t)$ are deterministic periodic functions with a period of one year, and $W(t)$ is a zero-mean, stationary, stochastic process. The functions $m(t)$ and $s(t)$ are seasonal mean value and seasonal standard deviation, respectively, and describe the exhibited seasonal patterns.

In order to properly treat variability at different time scales, the time series $Y(t)$ is re-indexed, using the following triple index notation:

$$\left\{ Y(j, m, \tau_k), \begin{array}{l} j = 1, \dots, J, \\ m = 1, \dots, 12, \\ k = 1, \dots, K_m \end{array} \right\}, \quad (2)$$

where j is the year index, m is the month index, τ_k represents the monthly time, and K_m is the number of observations within the m -th month. For example, for a time series with 3-hourly measurements, the number K_m for a month of 31 days is $8 \times 31 = 248$.

The three indices j , m , τ_k , represent three different time-scales, making it possible to explicitly define statistics with respect to each one of them separately. The subscripts: 1, 2, 3 are used to denote various statistics (mean value and standard deviation) with respect to the corresponding (first, second, third) index.

The seasonal patterns (mean value and standard deviation) are estimated by the following means:

1. The time series of monthly mean values and monthly standard deviations

are formed:

$$\mu_3(j, m) = \frac{1}{K_m} \sum_{k=1}^{K_m} Y(j, m, \tau_k), \quad (3)$$

$$\sigma_3(j, m) = \sqrt{\frac{1}{K_m} \sum_{k=1}^{K_m} [Y(j, m, \tau_k) - \mu_3(j, m)]^2}. \quad (4)$$

2. The seasonal patterns (mean value and standard deviation) are easily obtained by averaging the time series of Equations (3) and (4) over the years J :

$$\tilde{\mu}_3(m) = \frac{1}{J} \sum_{j=1}^J \mu_3(j, m), \quad (5)$$

$$\tilde{\sigma}_3(m) = \frac{1}{J} \sum_{j=1}^J \sigma_3(j, m), \quad (6)$$

with $m=1,2,\dots,12$. Stefanakos et al. (2006) have shown that, periodic extensions of quantities $\tilde{\mu}_3(m)$ and $\tilde{\sigma}_3(m)$ are good estimates of periodic functions $m(t)$ and $s(t)$.

Furthermore, if the residual component $W(t)$ is considered stationary, then the initial process $Y(t)$ forms the structure of a periodically correlated stochastic process.

Following the univariate case (1), a many-year long multivariate time series allows for the following decomposition:

$$\mathbf{Y}(t) = \mathbf{M}(t) + \mathbf{\Sigma}(t) \mathbf{W}(t), \quad (7)$$

$(N \times 1) \quad (N \times 1) \quad (N \times N) \quad (N \times 1)$

where N is the number of time series. The vector $\mathbf{M}(t)$ and the matrix $\mathbf{\Sigma}(t)$ are deterministic periodic functions with a period of one year, and $\mathbf{W}(t)$ is assumed to be a vector zero-mean, stationary, stochastic process. As in the univariate case, the functions $\mathbf{M}(t)$ and $\mathbf{\Sigma}(t)$ describe the exhibited seasonal patterns.

The terms of the seasonal patterns $\mathbf{M}(t)$ and $\mathbf{\Sigma}(t)$ are estimated following a procedure similar to the one used in the univariate case.

3. Fuzzy inference systems

Fuzzy theory was originally developed to deal with problems involving linguistic terms, like “tall” and “short” for height, “young” and “old” for age, etc (Zadeh, 1975a,b,c). Song & Chissom (1993b) defined fuzzy time series (FTS) and have applied the fuzzy time series model to forecast the enrollments of the University of Alabama (Song & Chissom, 1993a, 1994). Fuzzy sets are defined as sets whose elements have degrees of membership, in contrast to the classical theory, where the membership of elements in a set is considered in binary terms according to a bivalent condition.

Since then, various fuzzy time series models have been applied to the prediction of parameters from a plethora of problem areas such as stock market indices (Huarng, 2001b,a; Yu, 2005; Chen et al., 2007), temperature (Hsu et al., 2010), shipping market indices (Duru, 2010, 2012), and tourism (Tsaur & Kuo, 2011).

In the conventional set theory, the membership of an element x to a set L is characterized by the function

$$\mu_L(x) = \begin{cases} 1, & \text{if } x \in L, \\ 0, & \text{if } x \notin L, \end{cases} \quad (8)$$

The boundaries of such a set, and the set itself, are called crisp.

On the other hand, in fuzzy set theory a membership function can take several values between 0 and 1. Commonly used membership functions are: the triangular-shaped, the trapezoidal-shape, the bell-shaped etc.

All crisp sets can become fuzzy by assigning such a membership function. This procedure is called fuzzification.

Especially, if the membership function is of the form

$$\mu_L(x) = \begin{cases} \mu_L^-(x), & a_1 \leq x < a_2, \\ 1, & a_2 \leq x < a_3, \\ \mu_L^+(x), & a_3 \leq x < a_4, \\ 0, & \text{otherwise,} \end{cases} \quad (9)$$

where $\mu_L^-(x)$ is strictly increasing, and $\mu_L^+(x)$ strictly decreasing functions, respectively, then the associated fuzzy set L is called fuzzy number.

A conventional time series is considered as a realization of a random process. In the same sense, a fuzzy time series is considered as a realization of a a fuzzy random process; i.e., of a sequence of fuzzy random variables (Möller & Beer, 2008).

At each specific time instance t , the realization of each fuzzy random variable is a fuzzy variable; i.e., a collection of fuzzy numbers characterized by the collection of their membership functions defined in Equ. (9):

$$F(t) = \{\mu_{L_1}(t), \mu_{L_2}(t), \dots, \mu_{L_i}(t), \dots\} = \{\mu_1(t), \mu_2(t), \dots, \mu_i(t), \dots\} \quad (10)$$

If $F(t)$ is caused by $F(t-1)$, then there is a relationship of the form

$$F(t) = F(t-1) * R(t; t-1), \quad (11)$$

where '*' represents an operator. If $R(t; t-1)$ is independent of time t , then $F(t)$ is called a time-invariant time series. If $F(t-1)$ is associated with fuzzy set $L_{i,t-1} \equiv L_i$ and $F(t)$ with $L_{j,t} \equiv L_j$, then the relationship between $F(t)$ and $F(t-1)$ is also referred to as a fuzzy logical relationship (FLR), denoted by

$$L_i \rightarrow L_j, \quad (12)$$

where L_i is called the left-hand side (LHS) and L_j the right-hand side (RHS) of the FLR.

Fuzzy logical relationships can be further grouped into relationship group. Suppose there are FLRs with the same LHSs,

$$\begin{aligned} L_i &\rightarrow L_{k_1} \\ L_i &\rightarrow L_{k_2} \\ &\dots \end{aligned} \quad (13)$$

then, FLRs can be grouped into fuzzy logical relationship groups (FLRGs) of the form

$$L_i \rightarrow L_{k_1}, L_{k_2} \dots \quad (14)$$

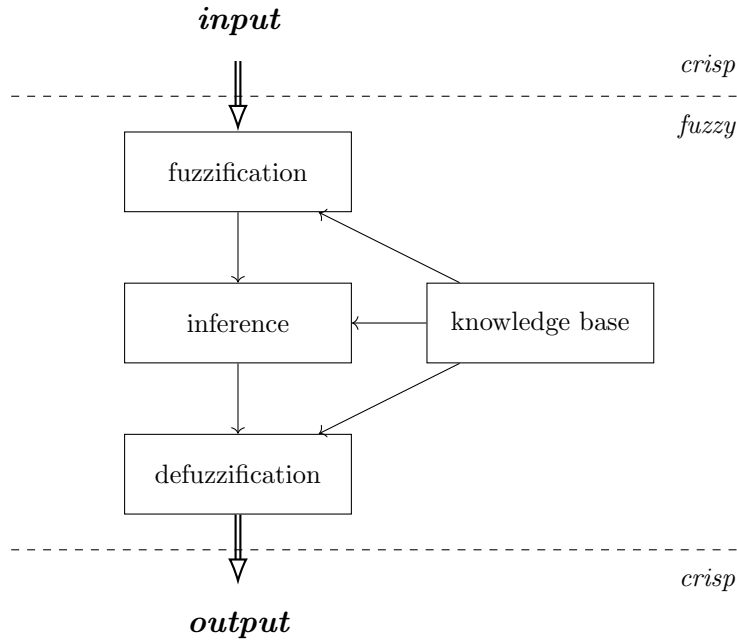


Figure 2: Sketch of fuzzy forecasting procedure

FLRs, which are also known as IF-THEN rules, are set up based on the experience of specialized experts from the available historical data. The first part of an IF-THEN rule is known as *antecedent* or *premise* and the second part as *consequent*.

Fuzzy Inference Systems (FIS) consist of the following building blocks; see also Fig. 2:

- (1) a *fuzzification* process, transforming the crisp values of the input;
- (2) a *knowledge base*, defining the appropriate membership functions and the IF-THEN rules based on available historical data;
- (3) an *inference* system, performing forecasts (inference) based on the established rules;
- (4) a *defuzzification* process, transforming the fuzzy forecasts back into crisp output.

There are two main types of Fuzzy Inference Systems, namely, the Mamdani

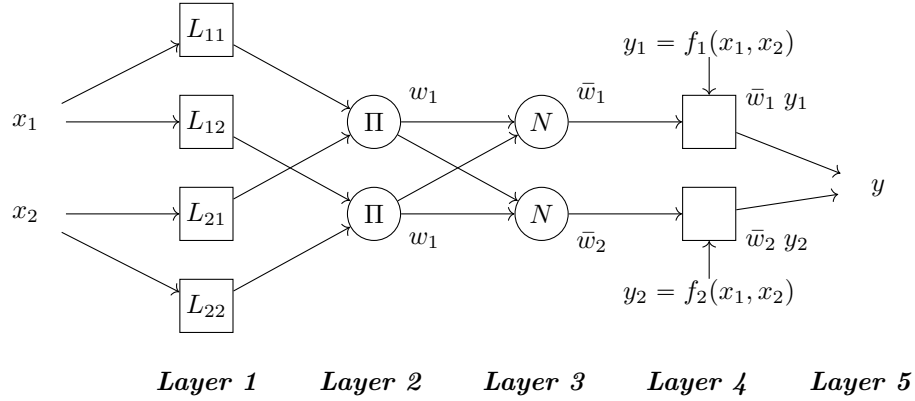


Figure 3: Sketch of ANFIS procedure

(Mamdani & Assilian, 1975) and the Takagi–Sugeno (TS) (Takagi & Sugeno, 1985), which mainly differentiates in the defuzzification process. In the Mamdani approach, each output belongs to a fuzzy set and needs defuzzification to obtain the crisp values of the output. The consequent part of the IF-THEN rules is of the form:

$$\begin{aligned}
 \text{Rule } k: \quad & \text{IF } W_S(t) \text{ is } \mathit{high} \text{ and } H_S(t) \text{ is } \mathit{high}, \\
 & \text{THEN } T_p(t+1) \text{ is } \mathit{high}, \quad k = 1, 2, \dots \quad (15)
 \end{aligned}$$

On the other hand, in the TS approach, the consequent part of each rule is a scalar expressed as a linear combination of the input variables of the form:

$$\begin{aligned}
 \text{Rule } k: \quad & \text{IF } W_S(t) \text{ is } \mathit{high} \text{ and } H_S(t) \text{ is } \mathit{high}, \\
 & \text{THEN } T_p(t+1) = p_k W_S(t) + q_k H_S(t) + r_k, \quad k = 1, 2, \dots, \quad (16)
 \end{aligned}$$

where p_k, q_k, r_k are parameters to be defined. The final value of the output variable is obtained by means of the weighted average of all IF-THEN outcomes.

Adaptive Network-based Fuzzy Inference Systems (ANFIS) were introduced by Jang (1993) and it is a TS FISystem where both antecedent and consequent parts are optimised based on the available data. The ANFIS procedure is illustrated by means of the following example; see also Fig. 3. Assume that we have a system with two inputs x_1, x_2 and one output y . The IF-THEN rules are of

the form

$$\text{IF } x_1 \text{ is } L_{1k} \text{ and } x_2 \text{ is } L_{2k}, \text{ THEN } y_k = p_k x_1 + q_k x_2 + r_k. \quad (17)$$

The ANFIS architecture consists of five layers:

Layer 1: The membership functions of the antecedent part are defined as

$$\mu_{L_i}(x) = \mu_{L_i}(x; a_i, b_i, c_i), \quad (18)$$

where a_i, b_i, c_i are called the parameters of the antecedent. The node is called adaptive, because it contains parameters which are to be estimated.

Layer 2: The weight of each rule k is calculated as

$$w_k = \mu_{L_{1k}}(x_1) \times \mu_{L_{2k}}(x_2). \quad (19)$$

This node is called fixed, since it does not contain parameters to be estimated.

Layer 3: The relative weight of each rule k is calculated as

$$\bar{w}_k = \frac{w_k}{\sum w_k}. \quad (20)$$

Layer 4: The output of each rule k is calculated as

$$\bar{w}_k y_k = \bar{w}_k f_k(x_1, x_2) = \bar{w}_k (p_k x_1 + q_k x_2 + r_k), \quad (21)$$

where p_k, q_k, r_k are parameters. This node is also adaptive, since it contains the parameters of the consequent part.

Layer 5: The final (weighted-average) value of the output is calculated as

$$y = \sum_k \bar{w}_k y_k. \quad (22)$$

The parameters of the consequent part are tuned in a forward propagation mode using least squares, while the antecedent parameters in a back-propagation learning algorithm (Jang, 1993).

Another important issue is the prevailing seasonal character of wind and wave time series, which calls for a nonstationary modelling of the series. In most

Fuzzy Time Series (FTS) studies, the nonstationarity is generally neglected and checking for stationarity is usually considered as an unnecessary condition for the FTS modelling. In contrast, Duru & Yoshida (2012), and the present author (Stefanakos et al., 2014), consider that nonstationarity should be first removed from the initial time series, before starting the fuzzy forecasting procedure. The reason is the following. Generally, FIS models use the pattern estimated based on the previous cases for the forecasting procedure. If the present step is a new condition that has never been experienced before, the so-called “no-change” solution is usually generated by the model as a forecasted value. So, if the forecasted time series end up to be a constant line, this is a strong indication of nonstationarity in the data.

4. Methodology

4.1. Data used

The data set used for this work consists of wave hindcasts done using the WAVEWATCH III model and GFS analysis winds. For more details, see Chawla et al. (2011). Although the hindcasts cover the entire globe with a half-degree resolution, we have used only the data cover the area shown in Fig. 4. At each datapoint, three-hourly time series of significant wave height H_S , peak wave period T_p and wind speed W_S are available. The time span of the data is 2005.02.01–2015.03.31, which is ten years and two months.

4.2. Model setup

For the prediction of wind speed W_S , significant wave height H_S and peak wave period T_p , the following FIS systems are assumed:

(a) wind speed W_S :

$$W_S(t+1) = f^{(1)}(W_S(t)) = p_k^{(1)}W_S(t) + s_k^{(1)}, \quad (23)$$

(b) significant wave height H_S :

$$H_S(t+1) = f^{(2)}(W_S(t), H_S(t)) = p_k^{(2)}W_S(t) + q_k^{(2)}H_S(t) + s_k^{(2)}, \quad (24)$$

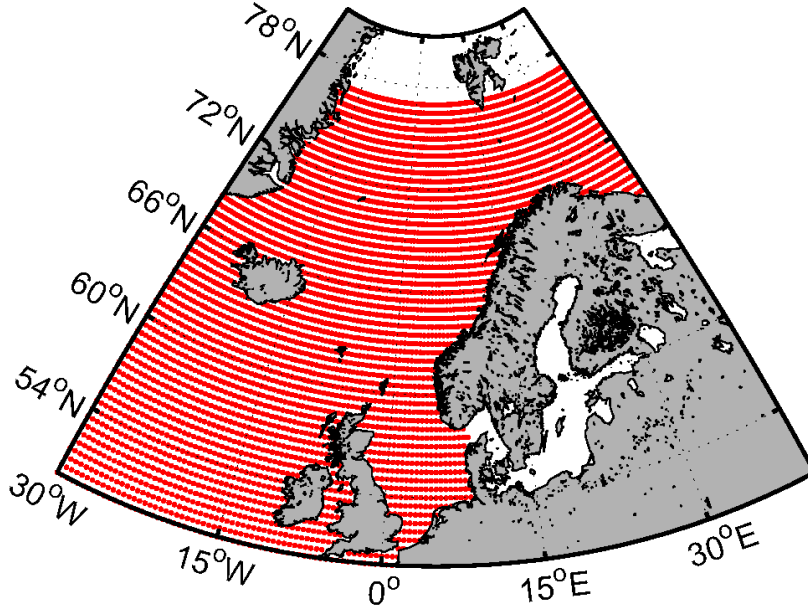


Figure 4: Data points used and covered area

(c) peak wave period T_p :

$$\begin{aligned}
 T_p(t+1) &= f^{(3)}(W_S(t), H_S(t), T_p(t)) = \\
 &= p_k^{(3)}W_S(t) + q_k^{(3)}H_S(t) + r_k^{(3)}T_p(t) + s_k^{(3)}, \quad (25)
 \end{aligned}$$

where the parameters $\{p_k^{(\cdot)}, q_k^{(\cdot)}, r_k^{(\cdot)}, s_k^{(\cdot)}\}$ in the above three equations are estimated using the ANFIS procedure described in Section 3.

The modelling of the membership functions has been intentionally kept as simple as possible in order to first depict the usability of the FIS/ANFIS methodology before proceeding to more sophisticated solutions. In that sense, two linear functions has been used for the membership functions of the fuzzy sets, representing the “Low” and “High” linguistic cases, respectively. In Fig. 5, an example of the membership functions is given for the case of significant wave height.

The number of rules is derived from the number of inputs in each one of the forecasting models (23)–(25). In Tables 1–3, one can find the values of the

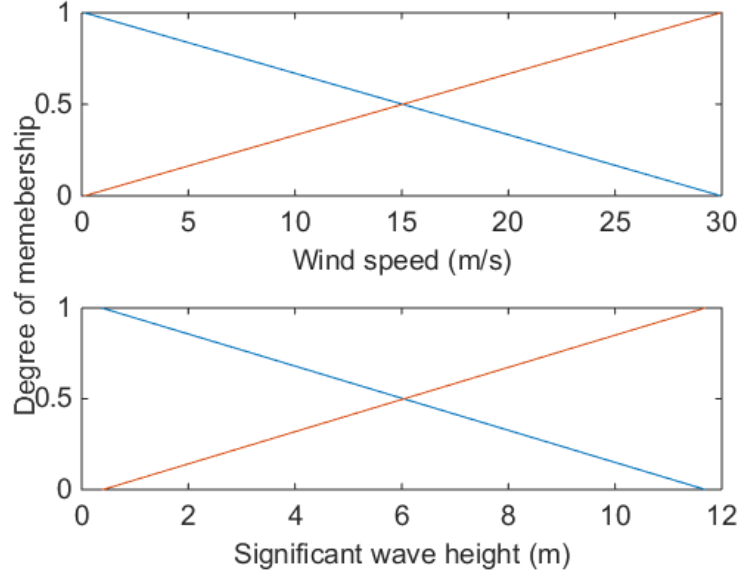


Figure 5: Membership functions of input variables for the case of significant wave height

Table 1: Fuzzy rules for the prediction of $W_S(t+1)$

	Input(s)	Output
Rule	$W_S(t)$	$W_S(t+1)$
1	Low	$1.0684 W_S(t) + 0.22669$
2	High	$0.85411 W_S(t) + 0.063187$

estimated parameters $\{p_k^{(\cdot)}, q_k^{(\cdot)}, r_k^{(\cdot)}, s_k^{(\cdot)}\}$, along with the IF-THEN rules implied for each case.

Of course, one may further improve the forecasts by experimentizing with the type and multitude of membership functions, and/or the multitude of IF-THEN rules. For example, in the present work, and for the sake of simplicity, all possible combinations of these rules have been considered. One, e.g., may a) increase the number of membership functions, b) keep only a subset of possible IF-THEN rules, c) use trapezoidal, Gaussian or user-defined membership functions, or d) combine all the above.

Table 2: Fuzzy rules for the prediction of $H_S(t + 1)$

Rule	Input(s)		Output
	$W_S(t)$	$H_S(t)$	$H_S(t + 1)$
1	Low	Low	$0.04005 W_S(t) + 0.73593 H_S(t) + 0.11531$
2	Low	High	$0.5966 W_S(t) + 0.47159 H_S(t) + 0.099497$
3	High	Low	$-0.0078906 W_S(t) + 0.17761 H_S(t) + 0.00056337$
4	High	High	$0.3224 W_S(t) + 0.17605 H_S(t) + 0.030245$

Table 3: Fuzzy rules for the prediction of $T_p(t + 1)$

Rule	Input(s)			Output
	$W_S(t)$	$H_S(t)$	$T_p(t)$	$T_p(t + 1)$
1	Low	Low	Low	$0.10368 W_S(t) + 0.35483 H_S(t) + 0.91832 T_p(t) + 0.063429$
2	Low	Low	High	$0.42497 W_S(t) + 0.33192 H_S(t) + 0.99617 T_p(t) + 0.07091$
3	Low	High	Low	$0.42499 W_S(t) + 0.25875 H_S(t) + 0.64724 T_p(t) + 0.050384$
4	Low	High	High	$0.42838 W_S(t) + 0.23776 H_S(t) + 0.62642 T_p(t) + 0.046257$
5	High	Low	Low	$-0.030458 W_S(t) + 0.12641 H_S(t) + 0.16931 T_p(t) + 0.0021683$
6	High	Low	High	$0.17572 W_S(t) + 0.14223 H_S(t) + 0.32119 T_p(t) + 0.019731$
7	High	High	Low	$0.29742 W_S(t) + 0.15283 H_S(t) + 0.32209 T_p(t) + 0.023884$
8	High	High	High	$0.29496 W_S(t) + 0.14547 H_S(t) + 0.33091 T_p(t) + 0.023932$

In the sequel, an example will be given to illustrate the forecasting procedure. Let us assume that, at time t , the values of wind speed and significant wave height are $x_1 = W_S(t) = 10$ m/s and $x_2 = H_S(t) = 2$ m, respectively. Based on the equations of the membership functions (MFs) given below (see also Fig. 5):

$$y_{\text{Low}}^{W_S} = -0.033535 x_1 + 1.004, \quad x \in [0.13, 29.95] \quad (26)$$

$$y_{\text{High}}^{W_S} = 0.033543 x_1 - 0.0046246, \quad x \in [0.13, 29.95] \quad (27)$$

$$y_{\text{Low}}^{H_S} = -0.088398 x_2 + 1.0335, \quad x \in [0.38, 11.69] \quad (28)$$

$$y_{\text{High}}^{H_S} = 0.088595 x_2 - 0.03557, \quad x \in [0.38, 11.69] \quad (29)$$

one can calculate the values of MFs for $x_1 = 10$ and $x_2 = 2$, which are given in Table 4. Further, using the rules given in Table 2, one can calculate the weight

Table 4: Values of membership functions for $W_S(t) = 10m/s$ and $H_S(t) = 2m$

	y_{Low}	y_{High}
W_S	0.66902	0.3308
H_S	0.85669	0.14162

of each rule based on Equ. (19):

$$w_1 = y_{\text{Low}}^{W_S} \times y_{\text{Low}}^{H_S} = 0.57315, \quad (30)$$

$$w_2 = y_{\text{Low}}^{W_S} \times y_{\text{High}}^{H_S} = 0.094747, \quad (31)$$

$$w_3 = y_{\text{High}}^{W_S} \times y_{\text{Low}}^{H_S} = 0.2834, \quad (32)$$

$$w_4 = y_{\text{High}}^{W_S} \times y_{\text{High}}^{H_S} = 0.046848, \quad (33)$$

and the forecasted values based on each rule:

$$y_1 = 0.04005 W_S(t) + 0.73593 H_S(t) + 0.11531 = 1.9877, \quad (34)$$

$$y_2 = 0.5966 W_S(t) + 0.47159 H_S(t) + 0.099497 = 7.0086, \quad (35)$$

$$y_3 = -0.0078906 W_S(t) + 0.17761 H_S(t) + 0.00056337 = 0.27688, \quad (36)$$

$$y_4 = 0.3224 W_S(t) + 0.17605 H_S(t) + 0.030245 = 3.6063. \quad (37)$$

Then, the forecasting of the final value $H_S(t+1)$ is performed using Equ. (22):

$$y = \frac{w_1 y_1 + w_2 y_2 + w_3 y_3 + w_4 y_4}{w_1 + w_2 + w_3 + w_4} = 2.0545 \text{ m}. \quad (38)$$

The forecasting procedure is applied both to the initial nonstationary time series $Y(t)$, and to the stationary part $W(t)$; see Equ. (1). The former procedure will be hereafter referred to as “ y -calculations”, and the latter as “ w -calculations”. Especially, in the latter, forecasts should be combined with the estimated $m(t)$ and $s(t)$, to obtain forecasts of the initial time series.

After the end of the prediction process, the forecasts based on w -calculations are compared against the ones obtained by the y -calculations. For this purpose, the dataset is divided into two parts: one for training and one for testing. Based on the latter dataset, various error measures are calculated and is the main tool for the comparison. The definition of these error measures is given in Section 4.3.

4.3. Measuring forecasting quality

Assuming that we have I steps of forecasts and actual values to be compared, there are three large categories of errors measuring the forecasting performance (Hyndman & Koehler, 2006):

- (i) *Scaled-dependent measures*, that depend on the scale of the data. These are useful when comparing different methods applied to the same dataset, but should not be used, for example, when comparing across data sets that have different scales.
- (ii) *Measures based on percentage errors*. Percentage errors have the advantage of being scale- independent, and so are frequently used to compare forecast performance across different data sets.
- (iii) *Relative measures*, which are calculated relatively to the error from a benchmark method.

Popular representatives of the first two categories are the

- (a) Root Mean Square Error (RMSE) defined as

$$\text{RMSE} = \sqrt{\frac{1}{I} \sum_{i=1}^I |e(t_i)|^2} \quad (39)$$

- (b) Mean Absolute Percentage Error (MAPE) defined as

$$\text{MAPE} = \frac{1}{I} \sum_{i=1}^I \left| \frac{e(t_i)}{\text{actual}(t_i)} \right|, \quad (40)$$

where

$$e(t_i) = \text{actual}(t_i) - \text{forecast}(t_i) \quad (41)$$

denotes the forecasting error at time t_i .

- (c) Percentage Error (PE) defined as

$$\text{PE}(t) = \frac{e(t)}{\text{actual}(t)}. \quad (42)$$

Results from the measures RMSE and MAPE are calculated and presented in Section 5 showing the accuracy of the proposed forecasting model.

Furthermore, Hyndman & Koehler (2006) coined the term “scaled error”, and they proposed that measures based on scaled errors should become the standard approach in comparing forecast accuracy.

A scaled error is defined as

$$q(t_i) = \frac{e(t_i)}{\frac{1}{N} \sum_{n=2}^N |X(t_n) - X(t_{n-1})|}, \quad (43)$$

where $\{X(t_n), n = 1, 2, \dots, N\}$ are the existing observations, used for training of the FTS model. Then, one can define various error measures in an analogous way. Let us consider, e.g., the

(a) Mean Absolute Scaled Error (MASE) defined as

$$\text{MASE} = \frac{1}{I} \sum_{i=1}^I |q(t_i)|, \quad (44)$$

and the

(b) Root Mean Square Scaled Error (RMSSE) defined as

$$\text{RMSSE} = \sqrt{\frac{1}{I} \sum_{i=1}^I |q(t_i)|^2} \quad (45)$$

Error measures MASE and RMSSE are also calculated and presented in Section 5.

Also, the usual error measures Bias, Scatter Index (SI) and correlation coefficient R^2 are calculated:

(a) Bias:

$$\text{Bias} = \frac{1}{I} \sum_{i=1}^I [-e(t_i)], \quad (46)$$

(b) Scatter Index (SI) in %:

$$\text{SI} = \sqrt{\frac{\text{RMSE}}{\sum_{i=1}^I \text{actual}(t_i)}} \times 100, \quad (47)$$

(c) Correlation coefficient R^2 :

$$R^2 = \frac{\sum_{i=1}^I \left(forecast(t_i) - \overline{actual} \right) \left(actual(t_i) - \overline{actual} \right)}{\sqrt{\sum_{i=1}^I \left(forecast(t_i) - \overline{actual} \right)^2 \sum_{i=1}^I \left(actual(t_i) - \overline{actual} \right)^2}}, \quad (48)$$

where

$$\overline{actual} = \frac{1}{I} \sum_{i=1}^I actual(t_i). \quad (49)$$

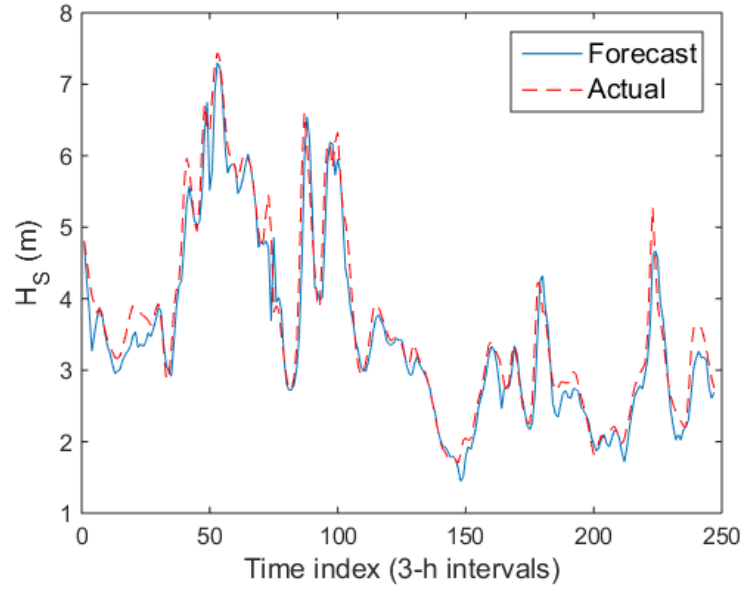
5. Numerical results and discussion

5.1. Point-wise forecast

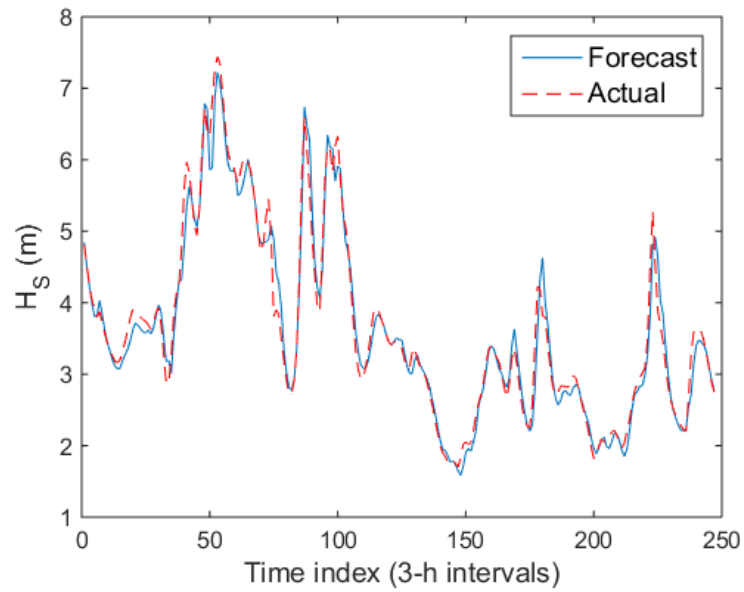
First, the forecasting procedure is applied and tested to wind and wave data for a point in the Norwegian Sea with coordinates (0 E, 63 N). The data consist of three-hourly time series of significant wave height H_S , wind speed W_S and peak wave period T_p . The total amount of datapoints (29688) is divided into two parts: one for training (29440) and one for testing (248). The values of the testing period correspond to one month data.

For the forecast of the three series, the methodology described in Section 4.2 is used, and the results are shown in Figs. 6–8 with a continuous line (“Forecast”). In the same figures, and for comparison purposes, the dataset kept for testing is plotted with dashed line (“Actual”). The (a)-part of the figures depict results based on the y -calculations, while the (b)-part results based on the w -calculations.

Then, the error statistics defined in Section 4.3 are calculated for all forecasts and are summarized in Table 5. According to this table, there is an improvement due to w -calculations which is reflected in the the reduction of the errors. This seems to be greater in significant wave height, where the error reduction is generally between 27-30% and with minimum and maximum values at 2% (R^2) and 82% (Bias), respectively. In wind speed the improvement is generally not so eminent (1%) with max value though at 56% (Bias). Finally, in peak wave period a mixed picture is present: some error measures are greatly improved

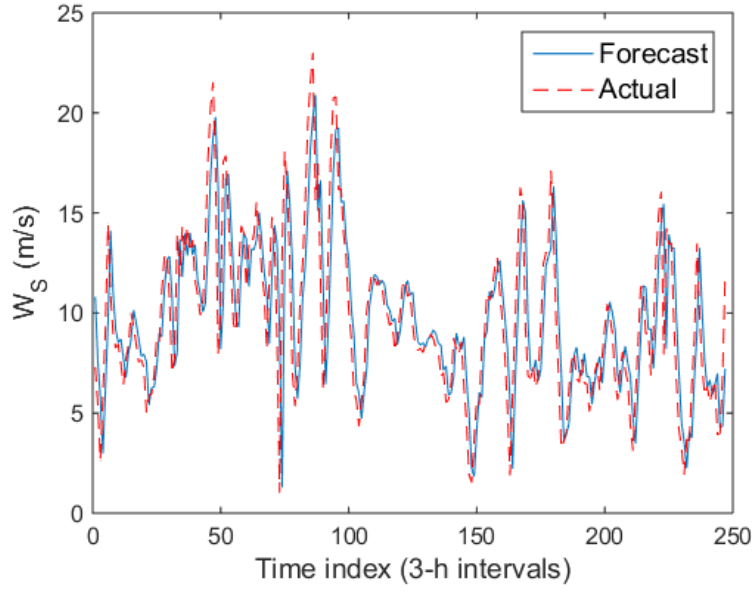


(a) y -calculations

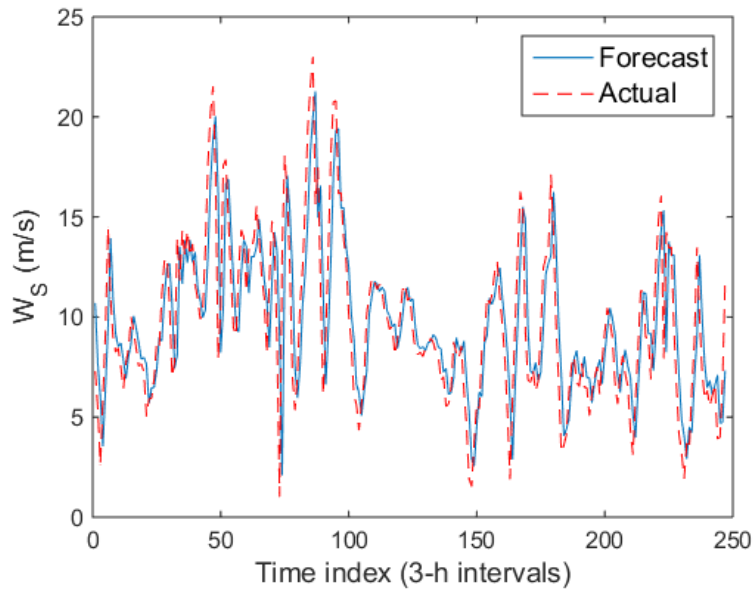


(b) w -calculations

Figure 6: Forecasts of significant wave height H_S

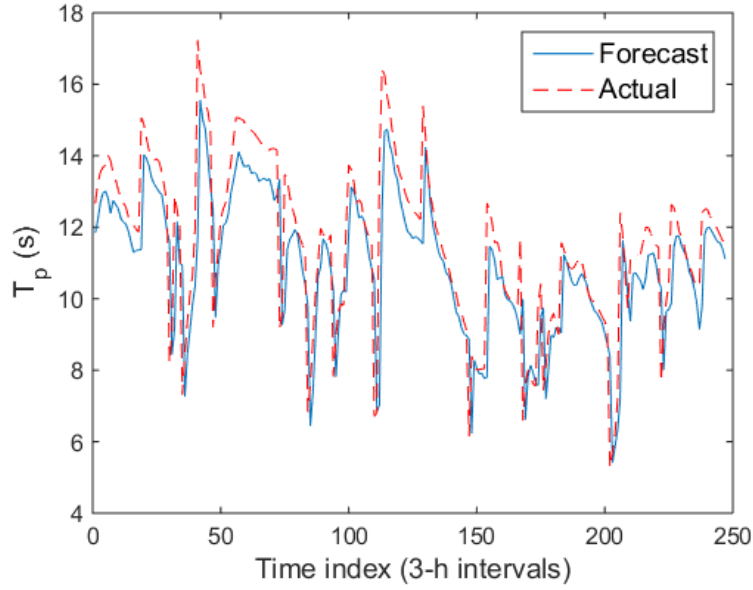


(a) y -calculations

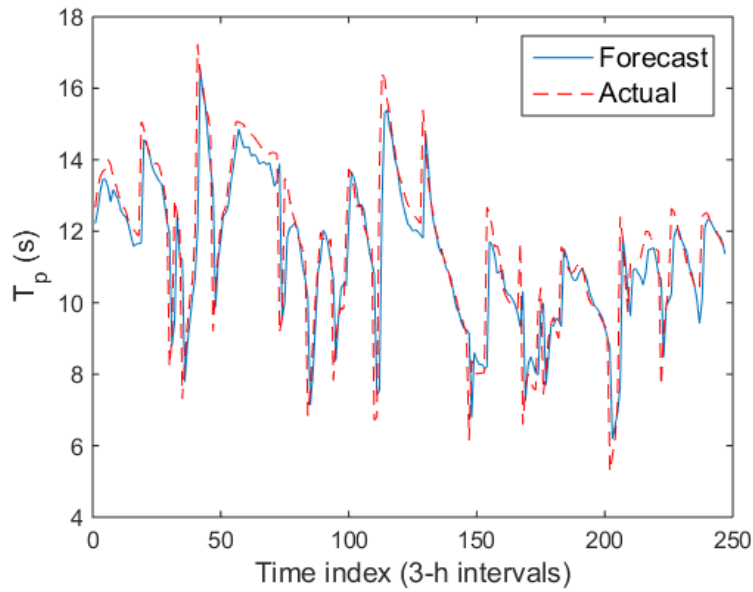


(b) w -calculations

Figure 7: Forecasts of wind speed W_S



(a) y -calculations



(b) w -calculations

Figure 8: Forecasts of peak wave period T_p

Table 5: Error measures

parameter	Bias	SI (%)	R^2	RMSE	MAPE	RMSSE	MASE
H_S (y -calc)	-0.162	9.052	0.968	0.331	0.063	1.492	1.062
(w -calc)	-0.029	6.588	0.983	0.241	0.045	1.086	0.747
W_S (y -calc)	0.048	26.089	0.790	2.531	0.258	1.315	0.985
(w -calc)	0.075	25.792	0.792	2.503	0.260	1.300	0.975
T_p (y -calc)	-0.605	12.100	0.792	1.400	0.085	1.937	1.295
(w -calc)	-0.232	10.980	0.829	1.271	0.067	1.758	0.966

(21-25%) while some others show a moderate improvement (5-9%) with max value of the improvement at 62% (Bias).

In the sequel, in order to further investigate the influence of the length of both the training and the testing period, the following two sensitivity investigations are performed.

First, the forecasting horizon has been kept fixed to 248 points (one month), and the error measures are calculated for various lengths of the training period. By inspecting Figs. 9–10, one can observe that in w -calculations the error measures are stabilised from the first point, which correspond to 1100 steps in the training set; approximately 4.5 times the forecasting period. On the other hand, in y -calculations the error measures are stabilised after 12000 steps, which roughly corresponds to 48 times the forecasting period. This example shows that, using w -calculations, not only error measures are reduced, but also less points are needed for the training period, which consist a clear improvement in the forecasting methodology.

In the second example, the forecasting horizon, and thus the points used in the testing period, varies from 124 (two weeks) to 7300 (two and half years). In Figs. 11–12, results based on both y - and w -calculations are given, depicting the better performance of the latter. Further, one may expect that the longer the forecasting horizon the higher the errors, which is not evident in these figures due to the averaging nature of the error measures.

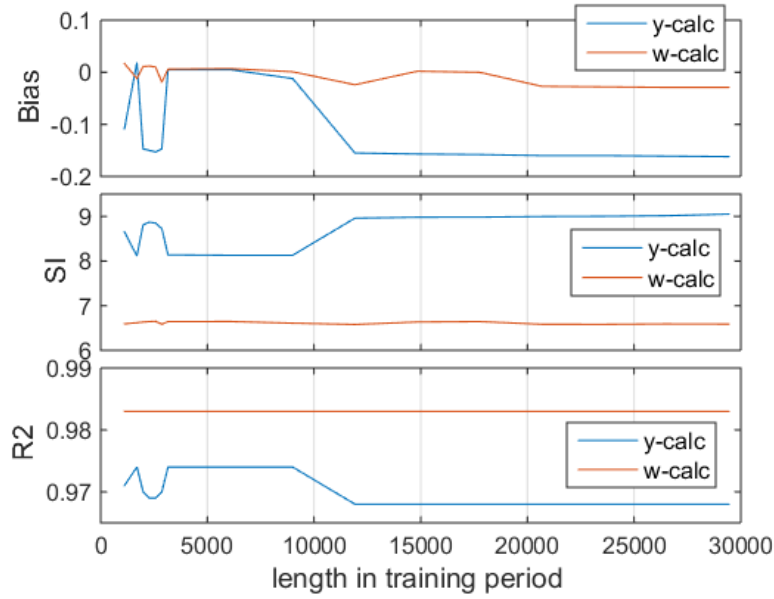


Figure 9: Error measures vs length in training period (Bias, SI, R2)

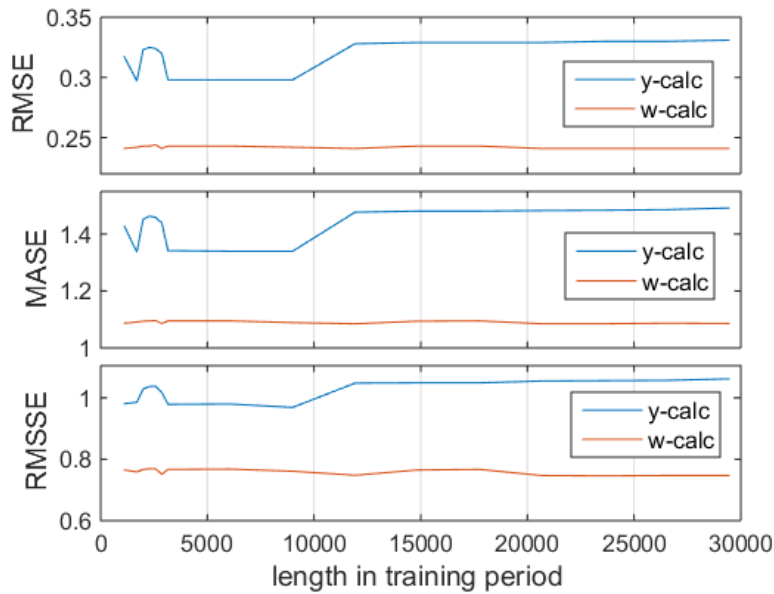


Figure 10: Error measures vs length in training period (RMSE, MASE, RMSSE)

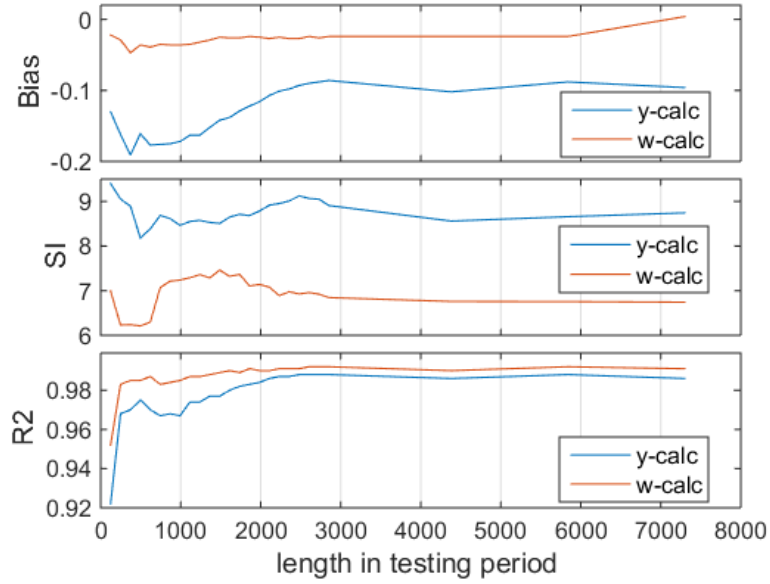


Figure 11: Error measures vs length in testing period (Bias, SI, R2)

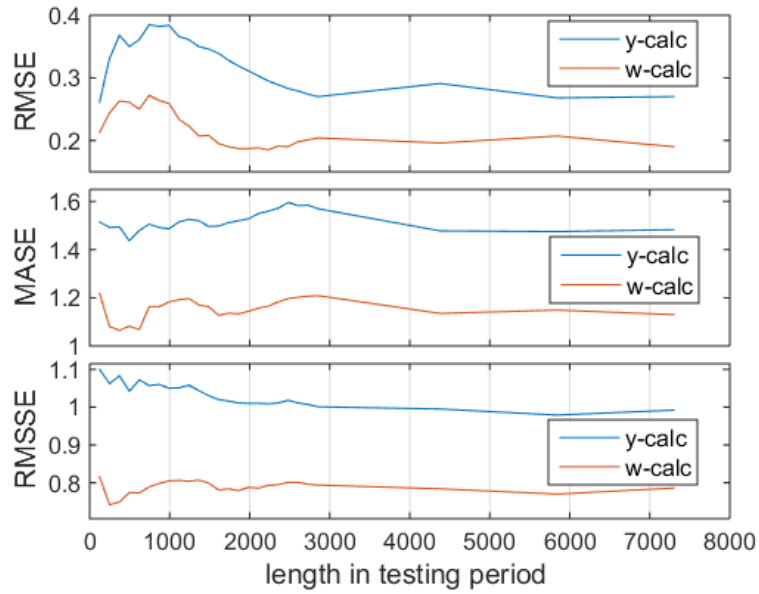


Figure 12: Error measures vs length in testing period (RMSE, MASE, RMSSE)

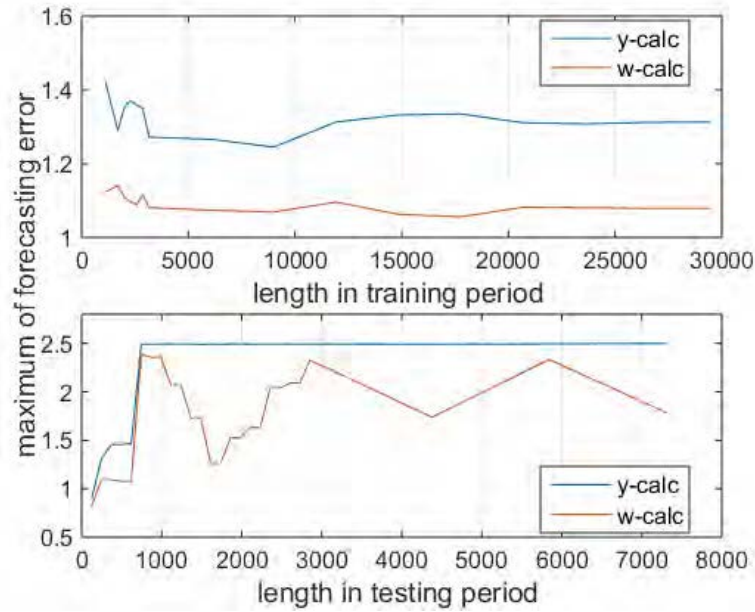


Figure 13: Maximum of absolute values of forecasting error vs length in (a) training, (b) testing period

In order to further investigate this, the maximum of absolute values of the instantaneous forecasting error (41) are calculated for various lengths of both the training and the testing period; see Figs. 13. In the upper figure, one can observe that these maximum errors are stabilized after a training length of approximately 5000, which corresponds to 1.7 years. According to the lower figure, in the forecasting of 124 points the max instantaneous error in both cases is near 0.8. However, after a length of 744 steps (3 months), the situation changes. On one hand, y -calculations' error becomes rapidly very high with values near 2.5 and is stabilized there. On the other hand, the corresponding curve of w -calculations depict an oscillating behaviour with peaks at 2.4 and troughs at 1.26 and 1.8. The better performance of the latter is attributed to an extent to the removal of the nonstationary character of the series before applying the forecasting procedure, a fact that allows the procedure to go on for longer forecasting horizons.

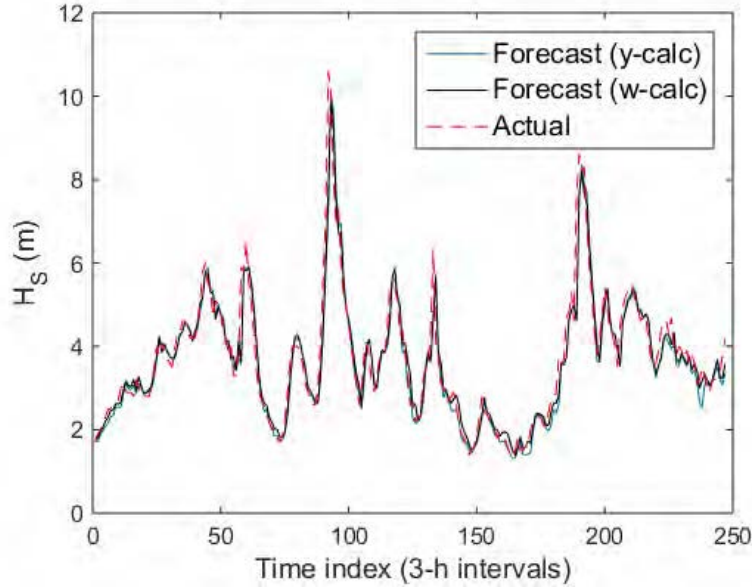


Figure 14: Forecasts of significant wave height H_S for Haltenbanken buoy

Table 6: Error measures for Haltenbanken forecasts

parameter	Bias	SI (%)	R^2	RMSE	MAPE	RMSSE	MASE
H_S (y -calc)	-0.104	14.179	0.939	0.525	0.084	1.415	0.893
(w -calc)	-0.028	13.237	0.946	0.490	0.082	1.321	0.848

Further, the same methodology is applied to measured wave data from Haltenbanken buoy in the Norwegian Sea (7.6 E, 65.1 N). The dataset consists of 3-hourly measurements of significant wave height, covering a period of 8 years (1980-1987). In Fig. 14, forecasted values are plotted with continuous lines and the testing dataset with dashed line. The associated error measures are given in Table 6, where once again lower errors suggest a better fit in the case of w -calculations.

Finally, the present (fuzzy) forecasting methodology has been assessed against other existing forecasting procedures in a previous work (Stefanakos et al., 2014), where the method has been compared against different ARIMA models of vari-

ous order.

5.2. Field-wise forecast

In the second application, forecasts are obtained for all the datapoints of the field shown in Fig. 4. According to Stefanakos (2008), after the extraction of the seasonal character from the initial time series, the remaining stationary W -part is almost stable in space. This fact can be exploited in order to accelerate the calculations for the field forecasts.

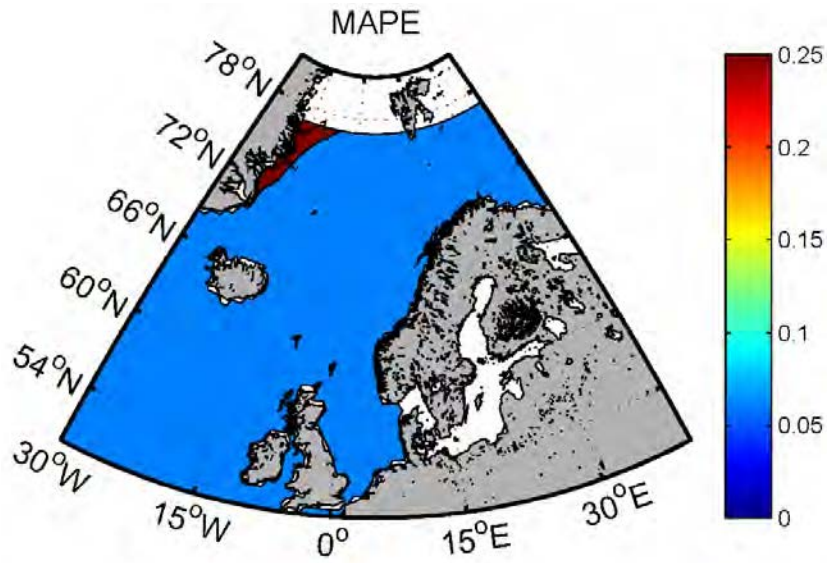
So, first, only one datapoint is considered and used for the fit of the FIS/ANFIS model. In our case, we have chosen the point lying in the bottom-left corner of our grid with coordinates (30 W,50 N), which is in the open sea and does not have any interactions with islands or depth-limited coastal areas. Then, the estimated ANFIS model from this point is applied to the W -parts of all other points of the field.

In this way, we have for comparison not only the 248 last points that we had in the previous case, but the whole series (29688 points). Thus, the various error measures, defined in Section 4.3, are much more reliable. In Figs. 15b,16b, 17b, 18b, MAPE, RMSE, MASE, RMSSE are depicted based on the w -calculations. For comparison purposes, the same quantities are shown in Figs. 15a,16a, 17a, 18a, based on the y -calculations.

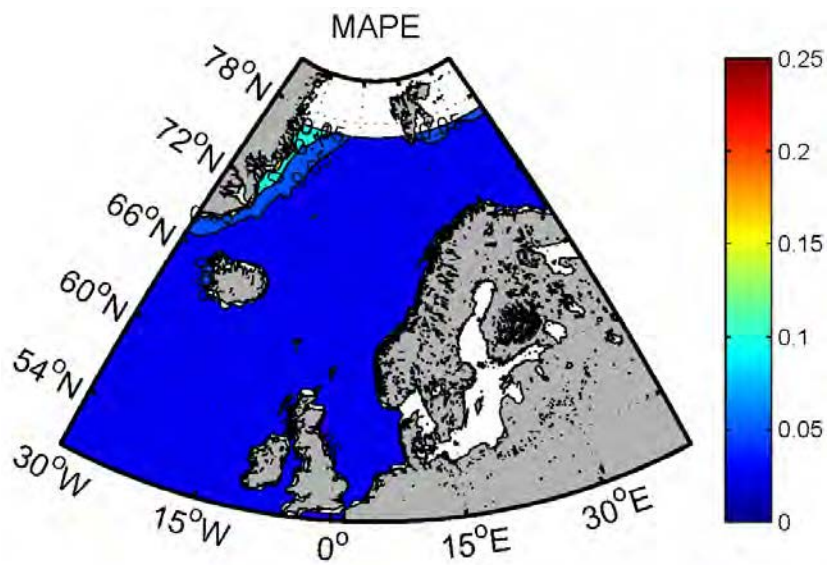
The comparison of these figures shows that the errors in w -calculations are lower than the corresponding ones in y -calculations. The mean value of the error reduction is a bit higher than 40% in RMSE and RMSSE, while it surpasses 50% in the cases of MAPE (55%) and MASE (65%).

This shows a great enhancement of the forecasting procedure by introducing the decomposition (1) and using only the stationary part of it. Also, the estimation of the ANFIS model using only just one point greatly accelerates the process of forecasting the field values.

Further, as in the point-wise case, the maximum of absolute values of the instantaneous forecasting error (41) are calculated for the whole field; see Figs. 19.

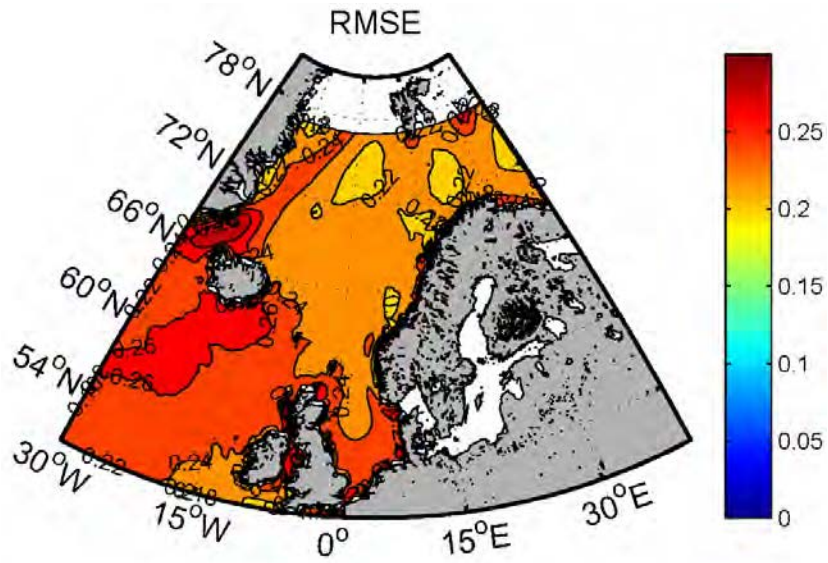


(a) y -calculations

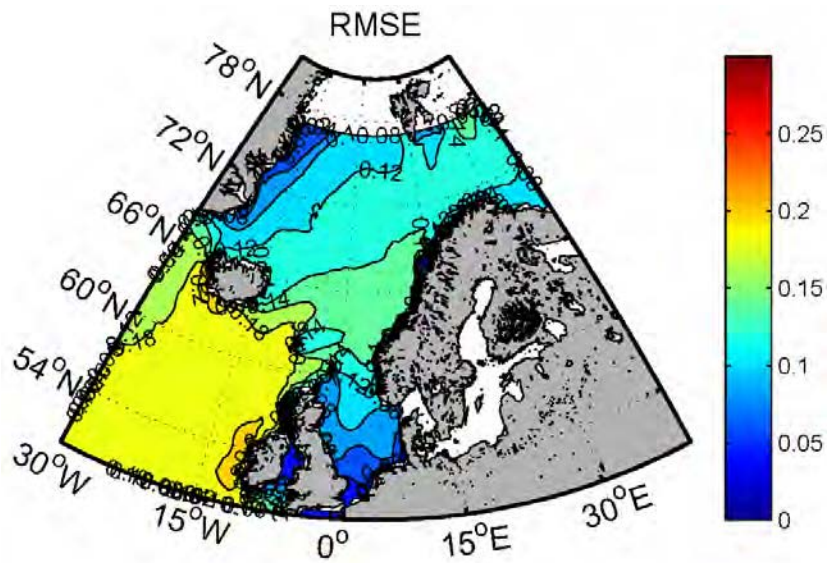


(b) w -calculations

Figure 15: Mean Absolute Percentage Error (MAPE)

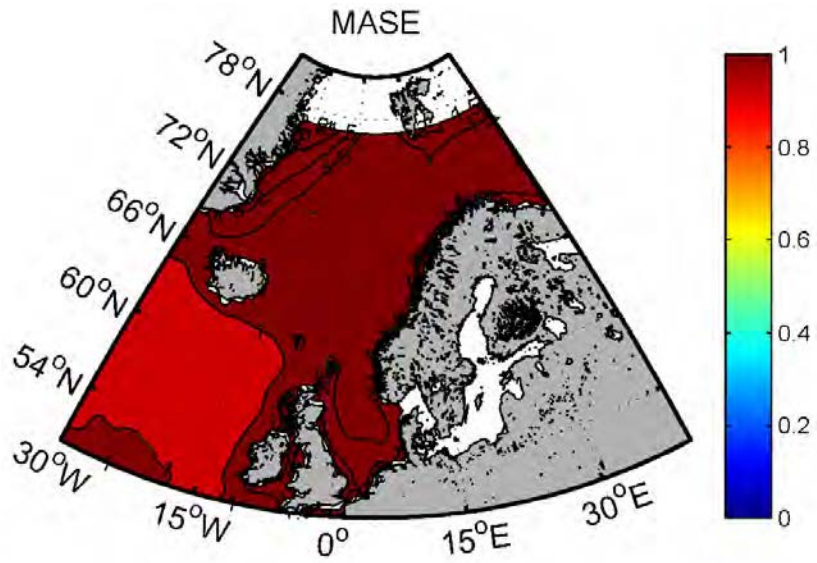


(a) y -calculations

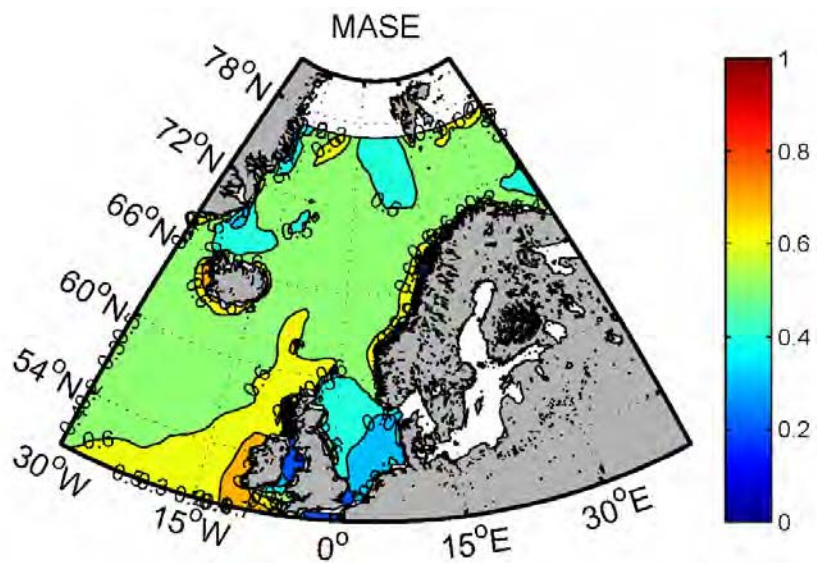


(b) w -calculations

Figure 16: Root Mean Square Error (RMSE)

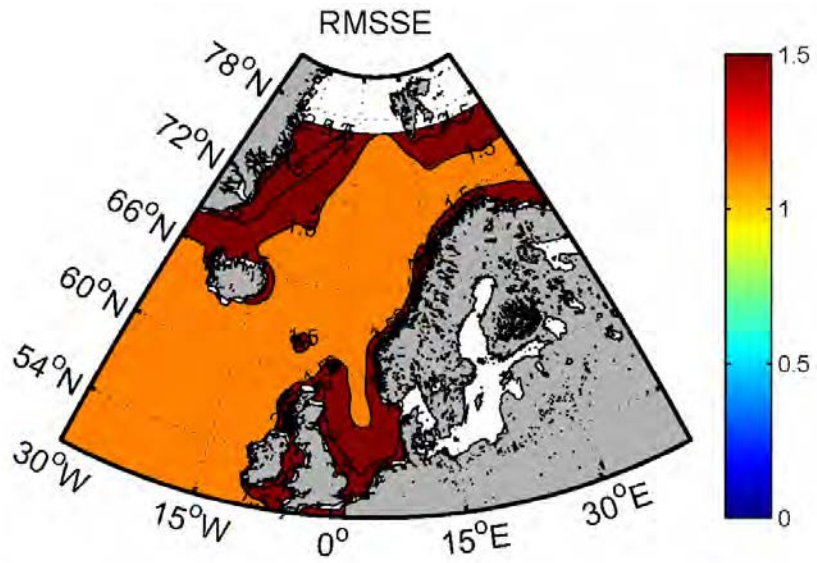


(a) y -calculations

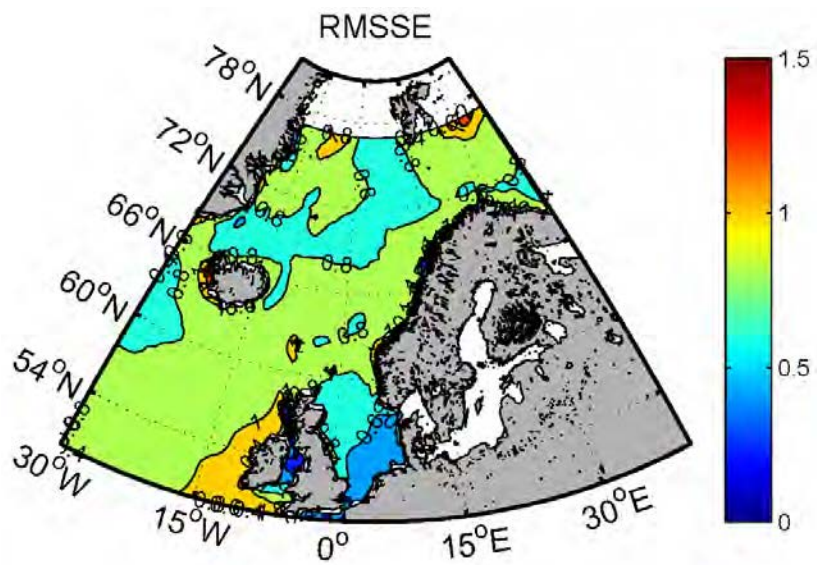


(b) w -calculations

Figure 17: Mean Absolute Scaled Error (MASE)

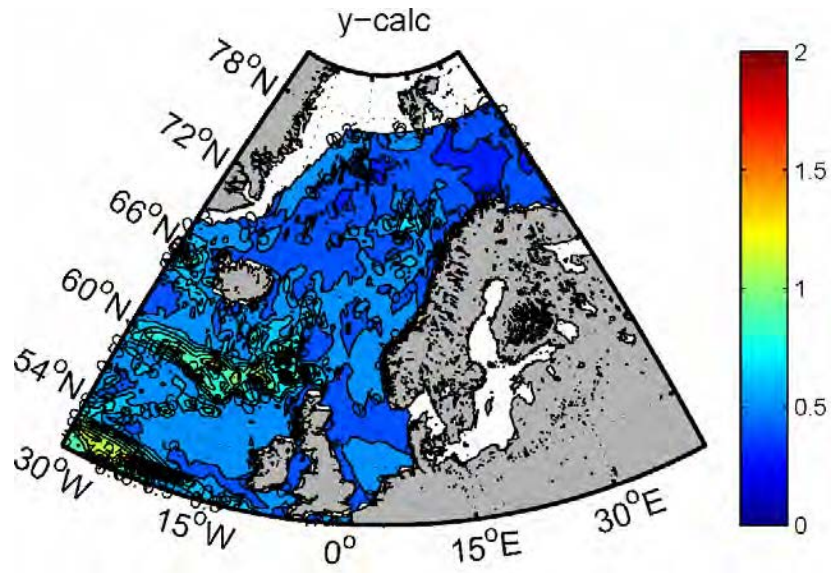


(a) y -calculations

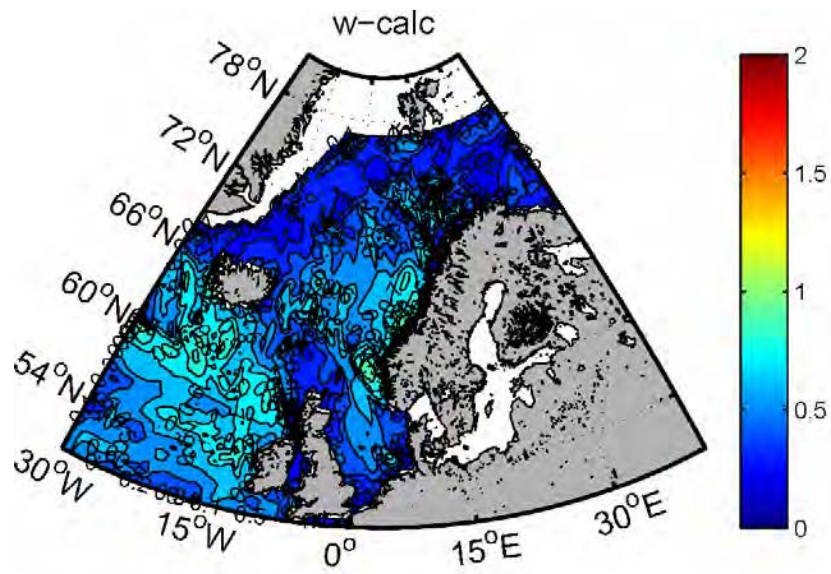


(b) w -calculations

Figure 18: Root Mean Square Scaled Error (RMSSE)



(a) y -calculations



(b) w -calculations

Figure 19: Maximum of absolute values of forecasting error

In the upper figure (y -calculations), one can observe that the maximum errors occur in the ocean area west of Ireland and south of Iceland. In contrast, in the lower figure (w -calculations), the pattern exhibits a great homogeneity with lower values of maximum forecasting error.

Finally, it is noteworthy to mention that the computational time needed for the y -calculations for the whole field was 2 days, while w -calculations took only 2.5 hours in a PC with Intel(R) Core(TM) i5-5200U CPU 2.20GHz and 4GB RAM.

6. Concluding Remarks

In the present work, forecasts of significant wave height H_S , peak wave period T_p and wind speed W_S for the area $[30W,40E] \times [50N,78N]$ have been obtained based on a newly introduced procedure.

The well-known Fuzzy Inference Systems (FIS) in combination with Adaptive Network-based Fuzzy Inference Systems (ANFIS) are coupled for the first time with a nonstationary time series modelling. This allows us to remove the nonstationary character of wind and wave time series before applying the forecasting techniques. It should be noted that, since the main purpose was to demonstrate the applicability of the coupling of the two methodologies, simple membership functions and IF-THEN rules have been chosen. Further work on optimal selection of these parameters is under way, and forecasts based on these improvements will be presented shortly.

The methodology is applied to obtain a) point-wise forecasts for a specific datapoint, and b) field-wise forecasts for the whole field of wave parameters. Especially, the latter is performed also for the first time.

For comparison purposes, the FIS/ANFIS models are also applied to the initial series without removing nonstationarity. The performance of both forecasting procedures is assessed by means of various error measures such as, e.g., Root Mean Square Error (RMSE), Mean Absolute Percentage Error (MAPE), Mean Absolute Scaled Error (MASE) and Root Mean Square Scaled Error (RMSSE).

The comparison of the error measures from the two approaches showed that the forecasts based on the proposed methodology outperforms the ones using only FIS/ANFIS models. Especially, in the case of the field-wise forecasts, the mean value of the error reduction is a bit higher than 40% in RMSE and RMSSE, and surpasses 50% in the cases of MAPE (55%) and MASE (65%).

Acknowledgments

This work has been partially funded by the NFR project “High-dimensional statistical modelling of changes in wave climate and implications for maritime infrastructure” (HDwave) under Contract No. 243814/E10, with partners Norsk Regnesentral (coordinator), DNV-GL and SINTEF Materials and Chemistry.

The author wishes also to thank anonymous reviewers for their fruitful comments that significantly improved the initial manuscript.

References

- Akpınar, A., Özger, M., & Kömörçü, M. I. (2014). Prediction of wave parameters by using fuzzy inference system and the parametric models along the south coasts of the Black Sea. *Journal of Marine Science and Technology*, *19*, 1–14. URL: <http://dx.doi.org/10.1007/s00773-013-0226-1>. doi:10.1007/s00773-013-0226-1.
- Athanassoulis, G., & Stefanakos, C. (1995). A nonstationary stochastic model for long-term time series of significant wave height. *Journal of Geophysical Research, Section Oceans*, *100*, 16149–16162. URL: <http://dx.doi.org/10.1029/94JC01022>. doi:10.1029/94JC01022.
- Booij, N., Ris, R., & Holthuijsen, L. (1999). A third-generation wave model for coastal regions: 1. model description and validation. *Journal of Geophysical Research, Section Oceans*, *104*, 7649–7666. URL: <http://onlinelibrary.wiley.com/doi/10.1029/98JC02622/full>. doi:10.1029/98JC02622.

- Chawla, A., Spindler, D., & Tolman, H. (2011). *WAVEWATCH III Hindcasts with Re-analysis winds. Initial report on model setup*. Technical Report National Centers for Environmental Prediction.
- Chen, T.-L., Cheng, C.-H., & Teoh, H. J. (2007). Fuzzy time-series based on fibonacci sequence for stock price forecasting. *Physica A: Statistical Mechanics and its Applications*, 380, 377 – 390. URL: <http://www.sciencedirect.com/science/article/pii/S0378437107001938>. doi:<http://dx.doi.org/10.1016/j.physa.2007.02.084>.
- Deo, M., Jha, A., Chaphekar, A., & Ravikant, K. (2001). Neural networks for wave forecasting. *Ocean Engineering*, 28, 889 – 898. URL: <http://www.sciencedirect.com/science/article/pii/S0029801800000275>. doi:[http://dx.doi.org/10.1016/S0029-8018\(00\)00027-5](http://dx.doi.org/10.1016/S0029-8018(00)00027-5).
- Duru, O. (2010). A fuzzy integrated logical forecasting model for dry bulk shipping index forecasting: an improved fuzzy time series approach. *Expert Systems with Applications*, 37, 5372 – 5380. URL: <http://www.sciencedirect.com/science/article/pii/S0957417410000217>. doi:<http://dx.doi.org/10.1016/j.eswa.2010.01.019>.
- Duru, O. (2012). A multivariate model of fuzzy integrated logical forecasting method (M-FILF) and multiplicative time series clustering: A model of time-varying volatility for dry cargo freight market. *Expert Systems with Applications*, 39, 4135 – 4142. URL: <http://www.sciencedirect.com/science/article/pii/S0957417411014461>. doi:<http://dx.doi.org/10.1016/j.eswa.2011.09.123>.
- Duru, O., & Yoshida, S. (2012). Modeling principles in fuzzy time series forecasting. In *2012 IEEE Conference on Computational Intelligence for Financial Engineering & Economics (CIFER)* (pp. 1–7). doi: 10.1109/CIFER.2012.6327767. URL: http://ieeexplore.ieee.org/xpls/abs_all.jsp?arnumber=6327767&tag=1. doi:10.1109/CIFER.2012.6327767.

- Hsu, L.-Y., Horng, S.-J., Kao, T.-W., Chen, Y.-H., Run, R.-S., Chen, R.-J., Lai, J.-L., & Kuo, I.-H. (2010). Temperature prediction and TAIFEX forecasting based on fuzzy relationships and MTPSO techniques. *Expert Systems with Applications*, *37*, 2756 – 2770. URL: <http://www.sciencedirect.com/science/article/pii/S0957417409007969>. doi:<http://dx.doi.org/10.1016/j.eswa.2009.09.015>.
- Huang, K. (2001a). Effective lengths of intervals to improve forecasting in fuzzy time series. *Fuzzy Sets and Systems*, *123*, 387 – 394. URL: <http://www.sciencedirect.com/science/article/pii/S0165011400000579>. doi:[http://dx.doi.org/10.1016/S0165-0114\(00\)00057-9](http://dx.doi.org/10.1016/S0165-0114(00)00057-9).
- Huang, K. (2001b). Heuristic models of fuzzy time series for forecasting. *Fuzzy Sets and Systems*, *123*, 369 – 386. URL: <http://www.sciencedirect.com/science/article/pii/S0165011400000932>. doi:[http://dx.doi.org/10.1016/S0165-0114\(00\)00093-2](http://dx.doi.org/10.1016/S0165-0114(00)00093-2).
- Hyndman, R. J., & Koehler, A. B. (2006). Another look at measures of forecast accuracy. *International Journal of Forecasting*, *22*, 679 – 688. URL: <http://www.sciencedirect.com/science/article/pii/S0169207006000239>. doi:<http://dx.doi.org/10.1016/j.ijforecast.2006.03.001>.
- Jain, P., & Deo, M. (2007). Real-time wave forecasts off the western indian coast. *Applied Ocean Research*, *29*, 72 – 79. URL: <http://www.sciencedirect.com/science/article/pii/S0141118707000417>. doi:<http://dx.doi.org/10.1016/j.apor.2007.05.003>.
- Jang, J.-S. (1993). ANFIS: adaptive-network-based fuzzy inference system. *Systems, Man and Cybernetics, IEEE Transactions on*, *23*, 665–685. URL: http://ieeexplore.ieee.org/xpls/abs_all.jsp?arnumber=256541. doi:10.1109/21.256541.
- Kazeminezhad, M., Etemad-Shahidi, A., & Mousavi, S. (2005). Application of fuzzy inference system in the prediction of wave parameters.

- Ocean Engineering*, 32, 1709 – 1725. URL: <http://www.sciencedirect.com/science/article/pii/S0029801805000533>. doi:<http://dx.doi.org/10.1016/j.oceaneng.2005.02.001>.
- Mahjoobi, J., Etemad-Shahidi, A., & Kazeminezhad, M. (2008). Hindcasting of wave parameters using different soft computing methods. *Applied Ocean Research*, 30, 28 – 36. URL: <http://www.sciencedirect.com/science/article/pii/S014111870800014X>. doi:<http://dx.doi.org/10.1016/j.apor.2008.03.002>.
- Mamdani, E., & Assilian, S. (1975). An experiment in linguistic synthesis with a fuzzy logic controller. *International Journal of Man-Machine Studies*, 7, 1 – 13. URL: <http://www.sciencedirect.com/science/article/pii/S0020737375800022>. doi:[http://dx.doi.org/10.1016/S0020-7373\(75\)80002-2](http://dx.doi.org/10.1016/S0020-7373(75)80002-2).
- Möller, B., & Beer, M. (2008). Engineering computation under uncertainty - Capabilities of non-traditional models. *Computers & Structures*, 86, 1024 – 1041. URL: <http://www.sciencedirect.com/science/article/pii/S0045794907002210>. doi:<http://dx.doi.org/10.1016/j.compstruc.2007.05.041>. Uncertainty in Structural Analysis - Their Effect on Robustness, Sensitivity and Design.
- Özger, M., & Şen, Z. (2007). Prediction of wave parameters by using fuzzy logic approach. *Ocean Engineering*, 34, 460 – 469. URL: <http://www.sciencedirect.com/science/article/pii/S0029801806001065>. doi:<http://dx.doi.org/10.1016/j.oceaneng.2006.03.003>.
- Rao, S., & Mandal, S. (2005). Hindcasting of storm waves using neural networks. *Ocean Engineering*, 32, 667 – 684. URL: <http://www.sciencedirect.com/science/article/pii/S0029801804002057>. doi:<http://dx.doi.org/10.1016/j.oceaneng.2004.09.003>.
- Reikard, G., & Rogers, W. E. (2011). Forecasting ocean waves: Comparing a physics-based model with statistical models. *Coastal Engineering*, 58,

- 409 – 416. URL: <http://www.sciencedirect.com/science/article/pii/S0378383910001821>. doi:<http://dx.doi.org/10.1016/j.coastaleng.2010.12.001>.
- Roulston, M., Ellepola, J., von Hardenberg, J., & Smith, L. (2005). Forecasting wave height probabilities with numerical weather prediction models. *Ocean Engineering*, *32*, 18411863. URL: <http://www.sciencedirect.com/science/article/pii/S0029801805000582>. doi:<http://dx.doi.org/10.1016/j.oceaneng.2004.11.012>.
- Song, Q., & Chissom, B. S. (1993a). Forecasting enrollments with fuzzy time series. Part I. *Fuzzy Sets and Systems*, *54*, 1 – 9. URL: <http://www.sciencedirect.com/science/article/pii/016501149390355L>. doi:[http://dx.doi.org/10.1016/0165-0114\(93\)90355-L](http://dx.doi.org/10.1016/0165-0114(93)90355-L).
- Song, Q., & Chissom, B. S. (1993b). Fuzzy time series and its models. *Fuzzy Sets and Systems*, *54*, 269 – 277. URL: <http://www.sciencedirect.com/science/article/pii/0165011493903720>. doi:[http://dx.doi.org/10.1016/0165-0114\(93\)90372-0](http://dx.doi.org/10.1016/0165-0114(93)90372-0).
- Song, Q., & Chissom, B. S. (1994). Forecasting enrollments with fuzzy time series. Part II. *Fuzzy Sets and Systems*, *62*, 1 – 8. URL: <http://www.sciencedirect.com/science/article/pii/0165011494900671>. doi:[http://dx.doi.org/10.1016/0165-0114\(94\)90067-1](http://dx.doi.org/10.1016/0165-0114(94)90067-1).
- Stefanakos, C. (2008). Investigation of the long-term wind and wave spectral climate of the Mediterranean Sea. *Proc. IMechE Part M: J. Engineering for the Maritime Environment*, *222*, 27–39. doi:DOI:10.1243/14750902JEME64.
- Stefanakos, C., Athanassoulis, G., & Barstow, S. (2006). Time series modeling of significant wave height in multiple scales, combining various sources of data. *Journal of Geophysical Research, Section Oceans*, *111*, 10001–10012. URL: <http://dx.doi.org/10.1029/2005JC003020>. doi:10.1029/2005JC003020.

- Stefanakos, C., & Belibassakis, K. (2005). Nonstationary stochastic modelling of multivariate long-term wind and watedata. In *24th International Conference on Offshore Mechanics and Arctic Engineering, OMAE'2005*. Halkidiki, Greece.
- Stefanakos, C., & Schinas, O. (2014). Forecasting bunker prices; a non-stationary, multivariate methodology. *Transportation Research Part C: Emerging Technologies*, *38*, 177 – 194. URL: <http://www.sciencedirect.com/science/article/pii/S0968090X13002453>. doi:<http://dx.doi.org/10.1016/j.trc.2013.11.017>.
- Stefanakos, C., Schinas, O., & Eidnes, G. (2014). Application of fuzzy time series techniques in wind and wave data forecasting. In *33rd International Conference on Offshore Mechanics and Arctic Engineering, OMAE'2014*. San Francisco, California.
- Sylaios, G., Bouchette, F., Tsihrintzis, V. A., & Denamiel, C. (2009). A fuzzy inference system for wind-wave modeling. *Ocean Engineering*, *36*, 1358 – 1365. URL: <http://www.sciencedirect.com/science/article/pii/S0029801809002182>. doi:<http://dx.doi.org/10.1016/j.oceaneng.2009.08.016>.
- Takagi, T., & Sugeno, M. (1985). Fuzzy identification of systems and its applications to modeling and control. *Systems, Man and Cybernetics, IEEE Transactions on, SMC-15*, 116–132. URL: http://ieeexplore.ieee.org/xpls/abs_all.jsp?arnumber=6313399&tag=1. doi:10.1109/TSMC.1985.6313399.
- Tolman, H. (1991). A third-generation model for wind waves on slowly varying, unsteady, and inhomogeneous depths and currents. *Journal of Physical Oceanography*, *21*, 782797. URL: <http://journals.ametsoc.org/doi/abs/10.1175/1520-0485%281991%29021%3C0782:ATGMFW%3E2.0.CO%3B2>. doi:[http://dx.doi.org/10.1175/1520-0485\(1992\)022<1095:EONOTP>2.0.CO;2](http://dx.doi.org/10.1175/1520-0485(1992)022<1095:EONOTP>2.0.CO;2).

Tsaur, R.-C., & Kuo, T.-C. (2011). The adaptive fuzzy time series model with an application to Taiwan's tourism demand. *Expert Systems with Applications*, 38, 9164 – 9171. URL: <http://www.sciencedirect.com/science/article/pii/S0957417411000790>. doi:<http://dx.doi.org/10.1016/j.eswa.2011.01.059>.

The WAMDI Group (1988). The WAM model-A third generation ocean wave prediction model. *Journal of Physical Oceanography*, 18, 1775–1810. URL: <http://journals.ametsoc.org/doi/abs/10.1175/1520-0485%281988%29018%3C1775%3ATWMTGO%3E2.0.CO%3B2>. doi:[http://dx.doi.org/10.1175/1520-0485\(1988\)018<1775:TWMTGO>2.0.CO;2](http://dx.doi.org/10.1175/1520-0485(1988)018<1775:TWMTGO>2.0.CO;2).

Yu, H.-K. (2005). Weighted fuzzy time series models for TAIEX forecasting. *Physica A: Statistical Mechanics and its Applications*, 349, 609 – 624. URL: <http://www.sciencedirect.com/science/article/pii/S0378437104014128>. doi:<http://dx.doi.org/10.1016/j.physa.2004.11.006>.

Zadeh, L. (1975a). The concept of a linguistic variable and its application to approximatereasoning–I. *Information Sciences*, 8, 199 – 249. URL: <http://www.sciencedirect.com/science/article/pii/0020025575900365>. doi:[http://dx.doi.org/10.1016/0020-0255\(75\)90036-5](http://dx.doi.org/10.1016/0020-0255(75)90036-5).

Zadeh, L. (1975b). The concept of a linguistic variable and its application to approximatereasoning–II. *Information Sciences*, 8, 301 – 357. URL: <http://www.sciencedirect.com/science/article/pii/0020025575900468>. doi:[http://dx.doi.org/10.1016/0020-0255\(75\)90046-8](http://dx.doi.org/10.1016/0020-0255(75)90046-8).

Zadeh, L. (1975c). The concept of a linguistic variable and its application to approximatereasoning–III. *Information Sciences*, 9, 43 – 80. URL: <http://www.sciencedirect.com/science/article/pii/0020025575900171>. doi:[http://dx.doi.org/10.1016/0020-0255\(75\)90017-1](http://dx.doi.org/10.1016/0020-0255(75)90017-1).

Zamani, A., Solomatine, D., Azimian, A., & Heemink, A. (2008). Learning from data for windwave forecasting. *Ocean Engineering*, 35, 953 – 962. URL: <http://www.sciencedirect.com/science/article/pii/S0029801808000632>. doi:<http://dx.doi.org/10.1016/j.oceaneng.2008.03.007>.